Depth Profiles of Polymer Mobility during the Film Formation of a Latex Dispersion Undergoing Photoinitiated Cross-Linking

M. Wallin,[‡] P. M. Glover,[†] A.-C. Hellgren,[‡] J. L. Keddie,[†] and P. J. McDonald*[,†]

Department of Physics, University of Surrey, Guildford, Surrey GU2 7XH, U.K., and Institute for Surface Chemistry, Box 5607, SE-114 86 Stockholm, Sweden

Received May 5, 2000; Revised Manuscript Received July 24, 2000

ABSTRACT: The first use of one-dimensional magnetic resonance imaging (MRI) to provide information on concentration and molecular mobility (as revealed by the spin−spin relaxation time, T_2) as a function of depth into cross-linking latex coatings during their film formation is reported. These materials are of interest because they provide hard, chemically resistant coatings and because, being waterborne, they do not release organic solvents into the atmosphere. MRI profiles, with a pixel resolution of 9 μm, are obtained at regular time intervals from a poly(vinyl acetate-*co*-ethylene) latex dispersion containing a difunctional cross-linker and a photoinitiator. In this complete formulation, MRI reveals that the rate of cross-linking is fastest in the middle regions of the coating. This result is explained by considering the combined effects of light scattering in the turbid latex, the inhibition of the free-radical cross-linking reaction by initial molecular oxygen, and the further ingress of oxygen from the atmosphere. A numerical model, using measured and known parameters, predicts MRI profiles that are in good qualitative agreement with those found experimentally.

1. Introduction

Latex film formation has been an active area of research for over 50 years.[2,3] Experimental and theoretical work have elucidated the fundamental mechanisms of the process. Significant progress has been made recently with the development of a model[4] that identifies the circumstances under which, for a given latex system, particle coalescence is driven by polymer/air, water/air, or polymer/water interfacial tensions. Now that film formation in conventional thermoplastic latex systems is becoming better understood, attention has shifted to film formation in reactive or cross-linking latex systems.[5,6]

Motivating this research is the need for hard, chemically resistant coatings that are waterborne (and accordingly do not release harmful volatile organic compounds (VOCs) into the atmosphere). Hard, chemically resistant polymers are obtained from a continuous cross-linked network. Hard thermoplastic latex particles (i.e., with a high glass transition temperature) can be cast onto a substrate but do not film-form at room temperature—at least without the use of coalescing aids that detrimentally release VOCs. Soft thermoplastic particles, on the other hand, *do* coalesce and interdiffuse readily but do not create a continuous, i.e., cross-linked, network. The use of cross-linking latex systems, in which cross-linking occurs during or after particle coalescence, overcomes the obstacles in obtaining hard, fully waterborne coatings at room temperature. That is, cross-linking polymers offer the specific advantages of enhanced mechanical strength, chemical resistance, and hardness in the final coating while enabling particle coalescence at room temperature without the release of VOCs.

Compared to film formation from thermoplastic latex particles, the film formation process in cross-linking systems is particularly complicated. First and foremost, the mechanical response of the polymer changes as a function of time in a cross-linking polymer, and so any description of the film formation process must take this fact into account. Second, the cross-linking reaction might not be spatially uniform (in depth or in lateral dimension). In cases in which cross-linking and particle coalescence are initiated at the air surface, a so-called "skin" layer may form.[7] Then, as has been observed in a non-cross-linking latex,[8] the drying rate is expected to decrease greatly, because water diffusion through a polymer is slower than through interparticle void space.[3] In the specific system studied here, the cross-linking is the result of a photoinitiated free-radical reaction. Consequently, one must consider the possible effects of oxygen inhibition of the free-radical polymerization, as has already been described in the literature for bulk systems.[9] Moreover, the photoinitiated reaction requires a certain minimum light intensity with specific wavelengths, but in a turbid latex, or in a latex that contains pigment, the light may not penetrate the entire depth of the coating, especially in the initial stages of drying.

The characterization of the film formation process requires a spatially resolved, discriminating, and noninvasive technique. Since its inception in 1973,[10,11] magnetic resonance imaging (MRI) has become the imaging modality of choice in numerous medical procedures. It has also been established as a valuable tool in materials science.[12] MRI is particularly well-suited for probing latex film formation, because it provides noninvasive analysis in the normal ambient atmosphere and at room temperature (or under a variety of other conditions). However, its previous application to film formation is very limited.

Previously, we showed that MRI analysis can determine the *lateral* diffusion rate of water during the drying of alkyd emulsions and a noncoalescing latex.[13] Here we turn our attention to *transverse* (i.e., vertical) nonuniformities in water concentration and in polymer mobility. We report the first use of a newly developed permanent magnet to perform MR profiling (one-

[†] University of Surrey.
[‡] Institute for Surface Chemistry.

10.1021/ma000787d CCC: $19.00
Published on Web 10/11/2000

dimensional imaging) during the film formation of latex films undergoing photoinitiated cross-linking. The new magnet arises from a recent advance in stray-field MRI[14] and offers a pixel resolution better than 10 μm in one-dimensional profiles of samples with a wide range of molecular mobilities. This resolution compares favorably to a typical pixel size on the order of 25 μm for mobile species using conventional MRI methods, which is clearly inadequate for the study of cross-linking in coatings that are only 100−200 μm thick.

In addition to compositional information, MRI provides spatially resolved measurements of molecular mobility. Specifically, the spin−spin relaxation time,[15] conventionally referred to as T_2, is intimately related to molecular motion, although the exact relationship between the two is not fully defined quantitatively, except through the introduction of molecular motion correlation times.[16,17] Qualitatively, liquids with low viscosity have a long relaxation time, whereas rubbers and polymer melts have shorter relaxation times. Glassy polymers have very short relaxation times, reflecting their rigid structure. The sensitivity of MRI to polymer mobility makes it ideal for the study of cross-linking systems in which there is a transition from a liquidlike state to a rubbery or solid state.

Various reaction strategies for chemical cross-linking have been reviewed elsewhere.[4,18] For maximum energy efficiency, it is desirable to cure latex systems at room temperature, although most systems studied to date, with only a few exceptions,[4] are thermally cured. One attractive way forward is through the exploitation of photoinitiated cross-linking. Curing of polymers with UV radiation was reported in the literature decades ago, and more recently researchers have investigated reactions initiated with visible light (comparable to solar radiation).[19,20] The initiation of free-radical polymerization via light-sensitive compounds has been well established in acrylic systems for use in dental applications.[21,22] One well-documented problem with the technology is the inhibition of the free-radical polymerization by the presence of molecular oxygen.[23] This problem is particularly serious in coatings because of the shorter length scales.[24]

The mechanisms of free-radical polymerization are well-documented, whereas little is known about the *spatial* variation of the reactions. In this work, we specifically determine how the extent and rate of cross-linking varies as a function of depth in a latex coating. We are aware of no other such measurements in the literature. We gain insight into the dependence of oxygen inhibition on distance from the sample surface. We draw upon kinetic descriptions of free-radical polymerization to develop a model to predict the extent of cross-linking in a latex film as a function of position. This model considers several effects: oxygen inhibition of cross-linking, light scattering in the turbid latex dispersion, diffusion of oxygen and water through the film, and water evaporation from the air surface. We interpret our MRI data in terms of the predictions of our model.

2. Experimental Details

2.1. Materials. The coatings formulation consists of three components: a latex dispersion, a cross-linker, and a photoiniator, which were mixed in a weight ratio of 10:2:0.1. The latex is based on a vinyl acetate/ethylene copolymer with a reactive aceto−acetoxy functionality. The dispersion has a broad particle size, with a mean value of 0.5 μm (according to photon correlation spectroscopy) and a solids content of 54 wt %. The cross-linker is a poly(ethylene glycol) diacrylate, which is a viscous, water-soluble liquid. Its difunctionality enables it potentially to react with neighboring polymer molecules to create a link between them. The proprietary photoinitiator was first dissolved in the cross-linker, and this solution was added dropwise to the latex dispersion while stirring. After thorough mixing, the formulation was left for a minimum of 1 day to allow air bubbles (created by the stirring) to be released.

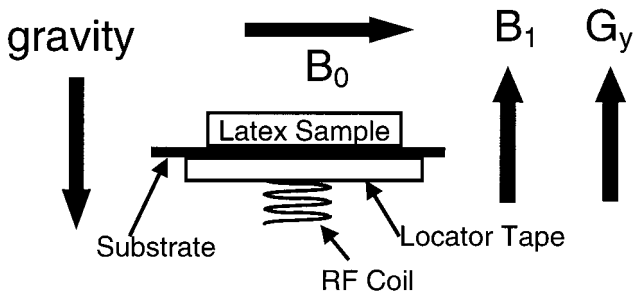

Figure 1. Schematic diagram of the experimental design used for magnetic resonance profiling. The sample is horizontal (i.e., perpendicular to the gravitational field) above a solenoidal radio-frequency coil used to excite and detect the NMR signal. The main magnetic field, $\mathbf{B_0}$, of 0.7 T acts in a direction parallel to the sample plane. The magnetic field due to the coil, $\mathbf{B_1}$, and the gradient in magnetic field, G_y (17.5 T m^{-1}), are perpendicular to the sample plane.

2.2. Methods. Coatings were cast on thin glass coverslips (with a surface area of 18 mm × 18 mm) that had been thoroughly cleaned with a surfactant solution (Decon-90) and hydrated by soaking in ethanol (to ensure full wetting). Typically the wet coatings were 200−300 μm thick. The relative humidity in the laboratory was not controlled but tended to be ca. 40%, and the average temperature was 23 °C. Cross-linking experiments were performed under a 575 W HMI lamp (with a color temperature of 6000 K). The distance between the lamp and sample surface was adjusted to ensure that the incident radiation was 1 mW cm^{-2}, as measured with a light meter.

Turbidity measurements were performed with a UV/vis spectrophotometer (CamSpec, Cambridge, UK). Coatings of varying thickness were sandwiched between coverslips, and optical transmissivity was measured. Gravimetric measurements of latex formulations drying in still air were conducted with a digital balance (AND HR-120) positioned under the HMI lamp such that the sample pan received a dose of 1 mW cm^{-2}. Measurements were made to the nearest 0.1 mg.

The MR profiles through the depth of the coatings were obtained with an imaging system incorporating a purpose-built, small permanent magnet. This magnet, described in detail elsewhere,[13] has specially shaped pole pieces that give a magnetic field of constant magnitude and nearly horizontal orientation in any horizontal plane around the central region. There is a strong gradient in the magnetic field strength in the vertical direction. At a position corresponding to a magnetic field of 0.7 T, the gradient strength is 17.5 T m^{-1}.

The latex samples, spread on the glass coverslips as already described, were placed flat into the field, as illustrated in Figure 1. Sample drying was always by free evaporation into the ambient still atmosphere of the laboratory. Because of the magnetic field gradient, hydrogen nuclei within the sample resonate with a frequency directly proportional to their vertical position (depth) in the film. The NMR signal is excited and then detected using a small solenoid sensor placed immediately beneath the sample. The excitation consisted of a multiple echo sequence:[25] $90_x-\tau-(90_y-\tau-\text{echo}-\tau-)_n$ with $n = 32$ echoes and a pulse gap of $\tau = 95$ μs. Each collected echo was individually Fourier transformed to yield a profile of the sample. The relative intensities for each echo of the profiles give information on the T_2 relaxation time for each plane. However, for our purposes, and to improve the signal-to-noise ratio of the accumulated data, it is sufficient to register and then sum the

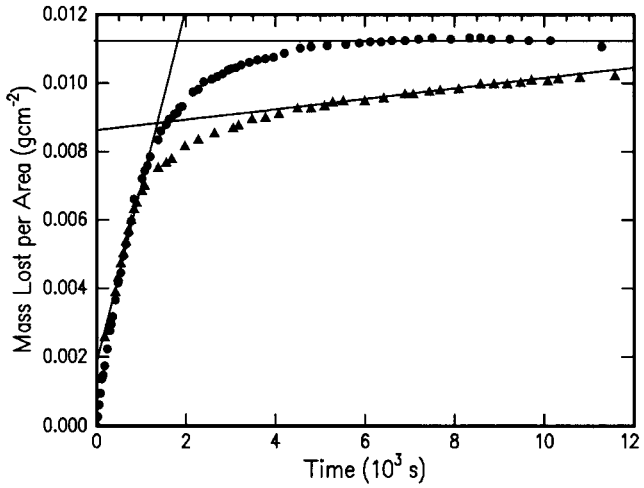

Figure 2. Comparison of the rate of water mass loss for a latex formulation with (▲) and without (●) added photoinitiator. The solid lines are the best fit to the data over small regions in time. For both samples, the initial water loss rate is ca. 5×10^{-6} g cm^{-2} s^{-1}. Without photoinitiator, the water loss rate reaches zero after about 5000 s.

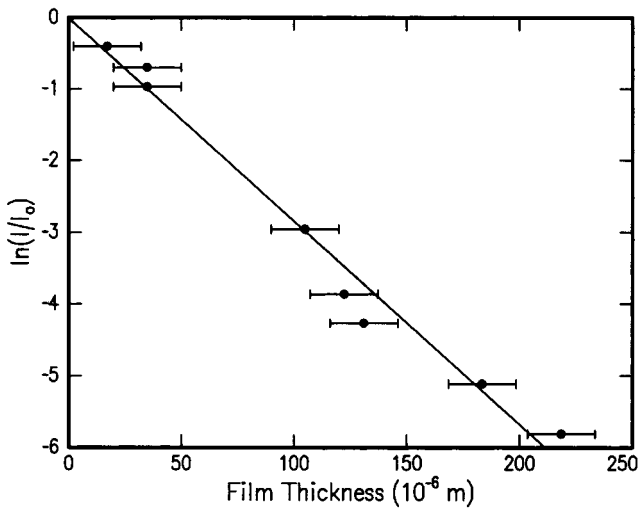

Figure 3. Transmitted intensity of light ($\lambda = 500$ nm) through wet layers of latex mixed with 20 w/w cross-linker as a function of film thickness. The curve of best fit corresponds to a characteristic length, z_0, of 40 μm in the Lambert equation (eq 9).

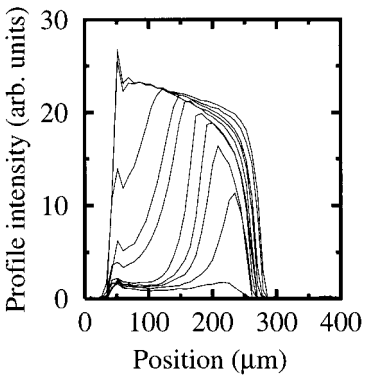

Figure 4. MR profiles recorded across a layer of cross-linker with photoinitiator exposed to light. The air surface is on the right; the substrate interface is on the left. The profile intensities have been normalized to a standard sample. From the top, they are recorded after 10, 90, 100, and 110 min and 2, 3, 4, 5, 6, and 17 h. Observe the close similarity between the first two profiles and the rapid onset of polymerization from the substrate interface thereafter.

profiles from the different echoes. For the chosen parameters, the nominal spatial resolution is 9 μm. Typically, 1024 averages were acquired in 5 min. The field of view of the profiles is limited by the spectrometer bandwidth. In consequence, the observed profile of a uniform layer is rounded. However, judicious positioning of the sample alleviates this problem to a very large extent. When necessary, the data were corrected for the drop in intensity associated with the spectrometer bandwidth limitation by normalizing to the profile of a uniform rubber sample. A layer of polymer tape was placed between the sensor and lower side of the sample substrate to act as a position reference. The reference is not shown in the results presented here.

3. Results

3.1. Characterization of Drying and Turbidity. The first results reported are the gravimetric analyses. Figure 2 shows experimental data for the mass loss of two samples of coating allowed to dry under the lamp: one with and the other without photoinitiator. In both, the mass loss rate is initially constant and is about 5×10^{-6} g cm^{-2} s^{-1}. This is close to the value of 4.3×10^{-6} g cm^{-2} s^{-1} for the evaporation of water into air with a relative humidity of 40%.[12,26,27] After about 30 min, the water loss rate slows, but differently in the two samples. In part, this slowing down is attributed to the reduction in surface areas of the coatings as they preferentially dry from the edges. In the latex without photoinitiator, there is no mass loss after about 1.5 h. In the film containing photoinitiator, on the other hand, there is continued mass loss well after 3 h. The water loss rate decreases significantly from the initial rate to about 2×10^{-7} g cm^{-2} s^{-1}, but it does not fall to zero, as is the case in the absence of photoinitiator. One interpretation of this simple gravimetric analysis is that the photoinitiator is creating a skin layer on the wet latex surface that slows down the evaporative water loss. There is indirect evidence that water is trapped within the coating underneath a cross-linked layer. Diffusion of water in the polymer is then much slower than in the interparticle void space.[3]

The turbidity measurements of the wet latex—needed to understand the spatial dependence of light intensity in the films studied with MR profiling—are considered next. Figure 3 shows measurements of light transmission through wet latex coatings as a function of thickness. The data show that the light intensity decreases exponentially with depth into the wet latex according to the Lambert equation and that the characteristic attenuation length is 40 μm. According to visual observations during MR and gravimetric analysis, the coating does not become completely transparent until all the water is lost.

3.2. MR Profiling. Each profiling experiment was designed to elucidate a different phenomenon: cross-linking, drying, and combined cross-linking and drying. In all of the MR profiles presented here, the intensity is a function of the mobile proton density, which, in turn, depends on the true proton density weighted by the molecular mobility. A preliminary experiment revealed that the neat cross-linker is able to react with itself to make a continuous network. Figure 4 shows typical profiles recorded for the cross-linker and photoinitiator alone when exposed to radiation under the lamp. The profiles clearly show the existence of an induction time of the order of 90 min during which there is no change in the profile intensity that would indicate polymerization. After this induction time, the intensity from the

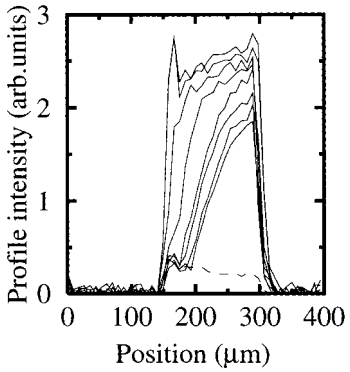

Figure 5. MR profiles recorded across a latex coating (complete formulation) exposed to light after having been dried in air for 1 day in the dark. The top profile is from the initial dried coating, immediately prior to switching on the light. Thereafter, the profiles from the top were recorded after 10 and 30 min and 1, 2, 3, 4, and 5 h. The light is incident on the air surface (i.e., the right-hand side of the figure). A final profile (dotted) was recorded after storage in darkness for a further 2 days, during which time the sample was removed from the magnet. This profile was separately normalized to the others at the lower edge.

cross-linker begins to decrease at the interface with the substrate. There is a strong spatial gradient in intensity, and this moves toward the air surface over time. These results are consistent with the cross-linker polymerizing fastest at the substrate interface.

A similar behavior is observed in a latex coating, shown in Figure 5, which consists of the complete latex formulation dried *in darkness* (to prevent photoinitiation) for 24 h in the normal ambient atmosphere *prior* to exposure to light during the MR profiling measurement. As the film is fully dry at the start of the analysis, all of the MR intensity is due to either the latex polymer or the cross-linker dissolved in it. These two components are not volatile, and the proton density of the layer presumably does not vary significantly with position and time. Any variation in intensity must therefore reflect changes in the cross-linker and polymer molecular mobility as a result of cross-linking. As also found with the neat cross-linker, the intensity decreases fastest along the interface with the substrate. This result can be explained by faster cross-linking there in comparison to near the air surface. The final profile has an intensity that is constant with depth, indicative of uniform cross-linking.

Next to be considered are the changes in MR profiles that accompany water loss by evaporation. Figure 6 shows the drying of a film cast from a latex dispersion (without cross-linker or photoinitiator) in air. There is a marked reduction in signal intensity over time accompanied by a reduction in the profile width. These changes are consistent with the evaporative loss of water from the coating. Initially, the intensity varies only slightly with depth in the sample, which indicates that the water concentration is likewise uniform with depth. At later times, the concentration is clearly much lower at the air surface; drying is inhomogeneous in the vertical direction. There is no evidence for a distinct skin layer. Gravimetric analysis of a similar, non-cross-linking sample (shown earlier in Figure 2) similarly suggests that there is no skin layer. When the film is fully dry, no NMR signal is obtained from the latex polymer.

Figure 7 shows profiles recorded to observe the drying of a latex dispersion containing cross-linker but no

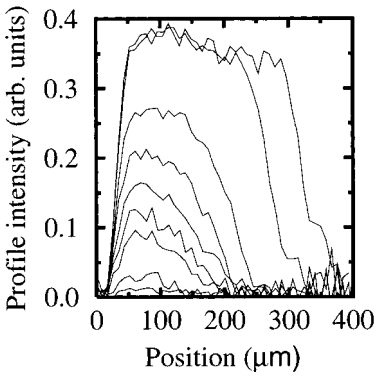

Figure 6. MR profiles recorded across a latex dispersion as it dries and film forms while in the magnet. The profiles (from the top) were recorded after 10, 20, 30, 40, 50, 60, 70, 100, and 120 min.

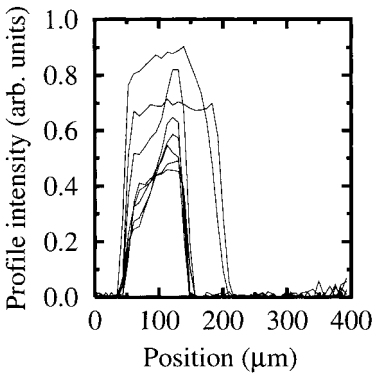

Figure 7. MR profiles recorded across a coating consisting of latex and 20 wt % cross-linker without photoinitiator as it dries and film forms. The first profile is the widest with a uniform intensity of about 0.7 au. The profiles then narrow and increase in intensity before once more falling in intensity. Observe how the later profiles pivot about the final almost square shape (intensity 0.4). The profiles were recorded after 5, 15, 25, 35 min and 1.0, 1.66, 2.83, and 4.08 h.

photoinitiator. The profiles start square and finish square, indicating a uniformity in concentration and molecular mobility with depth at the beginning and end of the drying process. The final profile intensity results from the cross-linker and plasticized latex. At intermediate times, however, the profile intensity *increases*, and there are reverse gradients in intensity such that the signal is reduced near the substrate. As in Figure 6, one might expect signal intensity to drop with water loss. Lower water concentration and thus a lower MR intensity might be expected at the air interface. These results are therefore contrary to expectation but are explicable in terms of changing magnetic resonance relaxation times as will be discussed in section 5.

Having examined the effects of cross-linking and water evaporation separately, the MRI profiles obtained from the complete latex formulation during film formation are now considered. Figure 8 shows the results obtained over time from such a coating under the lamp. The profiles reveal several important features. First, there is the expected overall loss of signal intensity over time due to both water loss and cross-linking reactions. (The first profile shown is typically of lower intensity than the second, but this is accounted for in terms of spin relaxation as discussed in relation to Figure 7 in section 5. Moreover, the first profile was recorded from a different sample due to instrumentation failure at the start of this long data acquisition run.) Second, there is

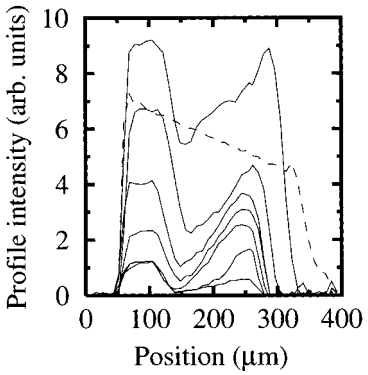

Figure 8. MR profiles recorded across a latex coating (complete formulation) exposed to light while drying in the magnet. Light is incident from the air side (on the right). The profiles were recorded after 10 min (dotted trace) and then, from the top, 30, 60, and 90 min and 2, 3, 6, and 17 h. The 10 min profile has a reduced intensity compared to the, say, 30 min profile, as a result of T_1-weighting in the intensity. (Note that due to instrumentation failure at the start of the long run, this particular profile was recorded from a separate coating.)

a shrinkage in film thickness due to the loss of water. Third, it is clear that the intensity decreases more slowly at the sample surface in comparison to the central region of the film. At all times shown, the intensity decreases fairly smoothly with depth into the sample. Fourth, along the substrate interface, the intensity is significantly higher. There is a rather abrupt step in intensity at a distance of about 75 μm from the substrate. The width of this bottom layer does not change much over time, but its NMR intensity decreases gradually. We speculate at this point that this rather complicated profile is the result of a combination of effects from cross-linking, oxygen inhibition, and light attenuation. To test these ideas, we next compare the experimental profiles to those obtained via numerical simulations.

4. Development of a Model of the Spatial Variation of Drying and Cross-Linking

The semiquantitative description of the experimental drying/cross-linking profiles developed here is based on four guiding principles. All four principles are consistent with experimental observations by us or others. The first is that the water is lost from the coating by liquid diffusion to the surface and thereafter by free evaporation. Since the latex used in this study is soft, we assume that particle coalescence is driven by capillary forces and therefore occurs simultaneously with water loss[3]. The second principle is that film formation proceeds by photoinitiated free-radical polymerization of the cross-linker molecule, which can react both with itself and with the latex polymer. Figure 3 showed that the incident light is attenuated exponentially by the turbid wet coating. It is thus assumed that the cross-linker molecules near the air surface are reacted more quickly than those further from the surface. However, the dry film is essentially transparent, and all layers are then irradiated equally. Third, it is supposed that the free-radical polymerization process is inhibited for the entire time that dissolved atmospheric oxygen remains in a particular layer. All samples start with a background concentration of molecular oxygen that is reduced at a rate equal to the free-radical production rate, due to an effectively instantaneous reaction with the free radical. Throughout the film formation process, a constant oxygen flux arrives at the film surface; oxygen diffuses in so as to obtain and maintain the equilibrium concentration. Last, a simple model relating the extent of cross-linking to the observed NMR signal intensity is incorporated. In the following sections, each of these principles is explained in greater detail.

4.1. Water Evaporation and Vertical Inhomogeneity. The loss of water from drops of aqueous coatings has been the subject of several recent studies. In general, it is observed that convex wet layers dry from the edges inward.[12,27,28] The necessary lateral transport of material is driven by gradients in concentration that are a natural consequence of a uniform water loss rate from a film of varying thickness.

The conditions for vertical homogeneity are less well understood and studied. There is some experimental evidence[6] for the formation of a so-called "skin layer" (a dry, coalesced layer at the surface over a wet interior), but it is not entirely convincing. Recently, Routh and Russel[3] devised a simple gauge to identify the conditions during which vertical homogeneity is expected. They suggest that the water concentration in the vertical direction is uniform when the relative rate of Brownian diffusion of the particles is greater than the water loss rate. The diffusion, which acts to equalize the water concentration, is described (for a dilute dispersion) by a coefficient D_0. This rate is expressed as the product of the evaporative flux, E (5×10^{-8} ms^{-1} in units of velocity), and the initial film thickness, H (typically 300 μm). That is, film uniformity during drying is obtained when $D_0/HE \gg 1$. The Brownian diffusion coefficient is given as $kT/6\pi\mu a$, where k is Boltzmann's constant, T is the absolute temperature (296 K), μ is the solvent viscosity (1×10^{-3} Pa s for water), and a is the particle radius (2.5×10^{-7} m for the latex studied here). For our latex, $D_0/HE \approx 0.06$, and so the concentration of water is not expected to be homogeneous in the vertical direction. In comparison, lateral homogeneity is a secondary effect. This prediction of inhomogeneity is consistent with the profiles observed for the neat latex in Figure 6.

Our simplified model therefore consists of a constant, maximum flux of water being removed from the film surface by free evaporation into (circulating) air. Hence, at the surface,

$$\frac{\partial \phi_w}{\partial t} = -E, \quad \phi_w > 0 \tag{1}$$

where ϕ_w is the water concentration and t is time. Loss of water from the surface leads to a vertical water concentration gradient that drives diffusion within the film, as described by Fick's second law,[30]

$$\frac{\partial \phi_w}{\partial t} = \frac{\partial}{\partial z}\left(D(\phi_w)\frac{\partial \phi_w}{\partial z}\right) \tag{2}$$

where z is the vertical position and D is the water diffusion coefficient. The problem arises, however, that the diffusion is not that of a single component in a pure second component. Rather, it is the *interdiffusion* of water, cross-linker monomer, cross-linker "polymer" (formed by reaction with itself or the latex), photoinitiator, latex particles, and oxygen. The general equation corresponding to Fick's first law for multicomponent

diffusion is[31]

$$F_i = \sum_{j=1} D^*_{i,j} \frac{\partial \phi_j}{\partial z} \tag{3}$$

where F_i is the flux of component i, ϕ_j is the concentration of component j, and $D^*_{i,j}$ is a multicomponent diffusion coefficient. In general, $D^*_{i,j} \neq D^*_{j,i}$ and not all the $D^*_{i,j}$ are mutually independent. For instance, for a ternary system, there are four independent coefficients and, in the case that $D^*_{i,j} = D^*_{j,i}$, only three. Several authors have attempted to rewrite this equation in terms of binary mixture diffusion coefficients. For instance, this can be done exactly for ideal dilute gases.[32] However, for complex dense systems such as this, the problem is much less tractable. We therefore adopt a model that arises from a Monte Carlo simulation in which diffusion occurs by pairwise exchange of components using an "atomistic" approach on a discretized lattice. The diffusion coefficient of component i in component j is expressed as $D_{i,j}$. It is readily shown that under such circumstances the flux of component i with respect to component j is given by

$$D_{i,j}\left(\phi_i \frac{\mathrm{d}\phi_j}{\mathrm{d}z} - \phi_j \frac{\mathrm{d}\phi_i}{\mathrm{d}z}\right) \tag{4}$$

where $D_{i,j} = D_{j,i}$, so that the effective diffusion equation pertaining to component i is

$$\frac{\partial \phi_i}{\partial t} = \sum_j D_{i,j}\left(\phi_j \frac{\partial^2 \phi_i}{\partial z^2} - \phi_i \frac{\partial^2 \phi_j}{\partial z^2}\right) \tag{5}$$

For a system of n components, this expression requires the definition of $(1 + 2 \ldots + (n - 1))$ diffusion coefficients. From eq 4, Fick's second law for the water in the latex formulation is given as

$$\frac{\partial \phi_\mathrm{w}}{\partial t} = \sum_j D_{\mathrm{w},j}\left(\phi_j \frac{\partial^2 \phi_\mathrm{w}}{\partial z^2} - \phi_\mathrm{w} \frac{\partial^2 \phi_j}{\partial z^2}\right) \tag{6}$$

Analogous equations can be written for the other components in the latex formulation.

4.2. Photoinitiated Free-Radical Polymerization. The precise details of the free-radical polymerization of the cross-linker and latex are not known. The fact that the cross-linker is dissolved in the latex serum but that it is moderately soluble in the latex particles adds further complication. It is known that the polymerization is initiated by light activation of the photoinitiator and that there is some similarity to the photopolymerization of methacrylate-based dental resins[20,21] and other acrylate systems.[23] Consequently, we adopt a generic model of free radical polymerization such as to be found in many standard texts.[33] The rate of free radical production is given by

$$v_i = \frac{\mathrm{d}[\mathrm{Q}^\bullet]}{\mathrm{d}t} = k_\mathrm{d} f\,[\mathrm{Q}] I \tag{7}$$

where k_d is the production rate constant, f is a factor describing the number of radicals generated per photon (i.e., the quantum yield), [Q] is the photoinitiator concentration, and I is the light intensity. In practice, the product $f\,I$ is assumed to be a single variable I. In the absence of inhibitor, and assuming, as is usual in such calculations, steady state-kinetics, then the overall rate of polymerization is given by

$$v_\mathrm{p} = \frac{\mathrm{d}[\mathrm{M_p}]}{\mathrm{d}t} = \frac{-\mathrm{d}[\mathrm{M}]}{\mathrm{d}t} = k_\mathrm{p}\left(\frac{k_\mathrm{d}[\mathrm{Q}]I}{k_\mathrm{t}}\right)^{1/2}[\mathrm{M}] \tag{8}$$

where [M] and [$\mathrm{M_p}$] are the monomer and polymer concentrations, respectively, and k_p and k_t are the propagation and termination rate constants, respectively. The difunctionality of the cross-linker is absorbed in the variable I.

As observed experimentally, the wet latex is highly turbid as a result of light scattering. A negligible amount of light can penetrate the full depth of the wet film. When substantial water evaporation proceeds, however, and particle coalescence takes place, light can penetrate the full depth of the film. It is assumed that in the wet, turbid film, light attenuation follows the Lambert equation:[34]

$$I = I_0 \exp(-z/z_0) \tag{9}$$

in which light with an initial intensity of I_0 has an intensity I at a depth z. The attenuation is hereby described by a characteristic length scale, z_0. When the film is fully dry, it is transparent and so $z_0 = \infty$. As a simplification, the gradual increase in z_0 over the drying time is neglected here.

4.3. Oxygen Inhibition. That oxygen acts as a scavenger of free radicals and thereby inhibits the free radical polymerization process is well-known.[22] It is possible to build the loss of free radicals due to oxygen scavenging into an enhanced scheme of rate equations, building on the theory presented in section 4.2. In practice, oxygen prevents cross-linking reactions and polymerization. For the purposes of our model, it is sufficient merely to remove any molecular oxygen from the system at a rate equal to the free radical production rate, as given in eq 6. Hence,

$$\frac{\mathrm{d}\phi_\mathrm{o}}{\mathrm{d}t} = -k_\mathrm{d} f\,[\mathrm{Q}] I, \quad \phi_\mathrm{o} > 0 \tag{10}$$

where ϕ_o is the concentration of dissolved molecular oxygen. Only when all of this oxygen is depleted, $\phi_\mathrm{o} = 0$, does the cross-linking (or polymerization) begin.

The dispersion presumably contains an initial level of dissolved oxygen when it is laid down. Of greater importance in explaining our experimental results, however, is the fact that additional oxygen ingresses into the latex film at a constant rate throughout the experiment. Therefore, it is also necessary for our model to consider the diffusion of oxygen into the film. This ingress is described with exactly the same mathematics used for the water. The change in oxygen concentration is then described as

$$\frac{\partial \phi_\mathrm{o}}{\partial t} = \sum_j D_{\mathrm{o},j}\left(\phi_j \frac{\partial^2 \phi_\mathrm{o}}{\partial z^2} - \phi_\mathrm{o} \frac{\partial^2 \phi_j}{\partial z^2}\right) - k_\mathrm{d} f\,[\mathrm{Q}] I + O \tag{11}$$

where the diffusive term operates throughout, the term $-k_\mathrm{d} f\,[\mathrm{Q}] I$ is included only while $\phi_\mathrm{o} > 0$, and the term describing the surface flux, $+O$, is included only at the surface and when $\phi_\mathrm{o} < \phi_\mathrm{o}^0$, the initial background oxygen concentration in the coating. The summation is over the remaining components: water, cross-linker,

reacted cross-linker, and latex polymer. In practice, it is likely that the oxygen flux will be time varying as, in a confined space, the oxygen above the sample will become depleted. We ignore this additional complication.

4.4. Spin−Spin Relaxation. The observed MR signal intensity is the sum intensity of a series of echoes resulting from the application of a sequence similar to the well-known Carr−Purcell−Meiboom−Gill pulse sequence.[24] The overall intensity of the signal is proportional to the sum of the individual volume fractions of the different chemical components (water, cross-linker, reacted cross-linker, and latex) at different locations, weighted by their respective hydrogen densities and molecular mobilities (through T_2 variations). As the hydrogen density does not vary greatly with component, and as the overall volume fraction remains unity, density variation is a poor discriminator of spatial variation in composition. However, since the T_2 of the liquid unreacted cross-linker and of the water (approximately 100 ms−1 s) are much greater than the chosen echo time of the experiment, while that of the reacted cross-linker and latex are much shorter (approximately 10−100 μs), mobility contrast is an excellent discriminator of composition. The former give rise to strong echoes, whereas the latter yield weak echoes.

Theoretical models linking T_2 to the extent of polymerization or cross-linking are not developed sufficiently to provide a quantitative, predictive relationship.[15,16] We use a simple phenomenological approach based on the experimental fact that the cross-linked polymer gives negligible measurable signal. The signal intensity derives solely from the mobile components. Separate measurements of pure water and of the dried latex containing 20 wt % cross-linker, under similar experimental conditions as used for the profiling, found that water yields an NMR signal intensity that is approximately twice that of the plasticized latex polymer and unreacted cross-linker per unit volume. The calculated intensity for a given composition is therefore taken as a weighted sum of the mobile component fractions.

4.5. Numerical Modeling. To reduce the problem to manageable proportions, the model was effectively simplified to just four components: (1) volatile water, (2) cross-linker, (3) reacted polymer (specifically taken as cross-linker reacted with itself and cross-linker reacted with the latex polymer), and (4) active molecular oxygen. The latex polymer was not considered as a separate component, but its volume fraction was included within that of the cross-linker, as a way of simplifying the model. Since the cross-linker is soluble in the latex polymer and is presumed to lead to cross-linking within it, this was not considered to be a serious oversimplification. The concentration of initiator was assumed at all times to be a constant fraction of the monomer and polymer. For ease of calculation, and without serious effect, deactivated oxygen was assigned to the polymer fraction. The diffusion coefficients were assumed to be independent of concentration.

The equations were solved using standard finite difference techniques**.** Time and space steps, δt and δz, were defined, and the initial concentrations of the four components were set uniform throughout the depth of the coating. The space step divided the coating into a series of layers. The calculation proceeded in a series of time loops during which the updated concentrations for each component, i, within each layer, j, at a time $t + \delta t$ (that, is $\phi_i{}^j(t + \delta t)$) were evaluated from the existing concentrations $\phi_i{}^{j-1}(t)$, $\phi_i{}^j(t)$, and $\phi_i{}^{j+1}(t)$. Each loop itself consisted of a series of steps. First, water was removed and oxygen added to the surface layer, according to eq 1 and the surface term of eq 11, respectively, to represent water evaporation and oxygen ingress. The new total sample volume was then calculated. The spatial step size, δz, and local concentrations of each component were accordingly revised by linear extrapolation between layers, so as to maintain total space filling of the sample. Next, the light intensity at each position was calculated for each layer, starting at the surface, using the differential form of eq 9. This was followed by a reaction step, during which either the active oxygen fraction—if greater than zero—was reduced (to represent oxygen inhibition) or—if the oxygen was entirely depleted—an appropriate fraction of cross-linker was converted to reacted polymer, according to eq 8, using the light intensity at the relevant depth. Finally, a diffusion step was performed in which the concentration of each component in each layer was updated according to eq 5 in order to reduce any spatial concentration gradients.

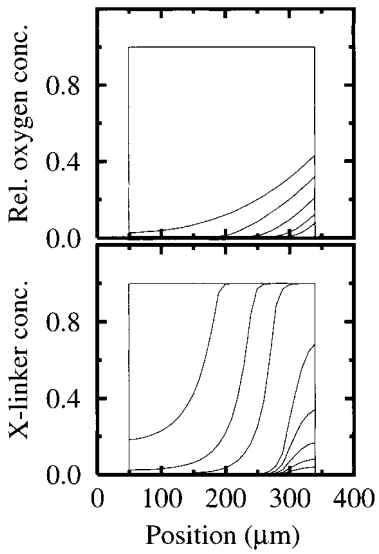

Figure 9. Simulated profiles for the cross-linking of a layer comprising just cross-linker and photoinitiator, using the parameters given in the text. The top plot shows the active oxygen as a fraction of the initial background oxygen; the bottom plot shows the fraction of unreacted cross-linker which mimics the magnetization intensity. Profiles are shown for 0, 84, 96, and 108 min and then 2, 3, 4, 5, 6, and 7 h, comparable to the times shown in Figure 4. In the upper figure the oxygen concentration reaches a steady state at longer times, while in the lower figure the first two profiles overlay each other. Light is incident from the right.

5. Numerical Analysis

Simulations were conducted to predict the time-dependent MR profiles for the cross-linker and photoinitiator alone exposed to light (Figure 9), for the drying of the latex dispersion in the absence of cross-linker and photoinitiator (Figure 10), and for the complete latex formulation exposed to light (Figure 11). These simulations are meant to be compared to the experimental results in Figures 4, 6, and 8, respectively. The initial concentrations of the four components for each simulation are based on the experimental formulations and are given in Table 1.

The upper part of Figure 9 shows periodic concentration profiles of active oxygen in a cross-linker/photoini-

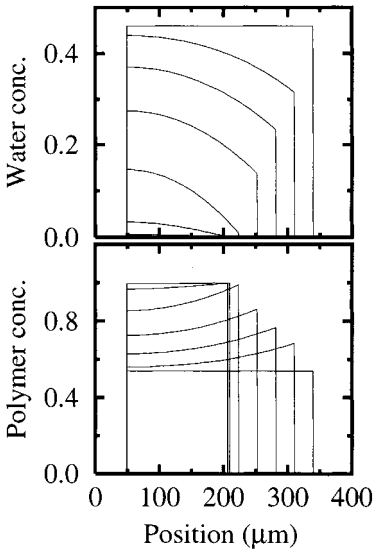

Figure 10. Simulated profiles for a latex dispersion as it dries and film forms while in the magnet. The profiles are shown at 10 min intervals, starting from time zero. The top plot shows water concentration decreasing and the film thickness shrinking. The lower plot shows the corresponding increase in the latex polymer concentration. The upper plot mimics the magnetization (cf. Figure 6).

tiator mix exposed to light. The initial profile is spatially uniform. With time, the active oxygen concentration is depleted by the photoinduced free radicals, but near the air surface, the concentration is replenished by oxygen diffusion. These oxygen profiles result in the profiles in the lower part of Figure 9, which show the unreacted monomer fraction. It does not change from the initial square profile shape during the first 30 min as a result of oxygen inhibition of the reaction. However, as soon as the oxygen concentration reaches zero along the substrate interface, the cross-linker starts reacting. A polymerization front proceeds upward through the film. The surface region cross-links last and is not fully cross-linked for several hours. Critical to this simulation is the diffusion of cross-linker monomer in the "polymer" (i.e., cross-linker reacted with itself). The surface oxygen concentration never reaches zero but rather attains a steady state concentration. In the absence of cross-linker diffusion, therefore, cross-linking would be perpetually inhibited at the surface. The cross-linker diffusion in the polymer, however, ensures that cross-linking occurs even at the surface, albeit slowly. According to the simple model, the expected magnetization is proportional to the unreacted cross-linker content, and so the lower part of Figure 9 can be compared directly to Figure 4. A general correlation is seen between theory and experiment. Note in particular that, in both, the profiles move away from the substrate and then decrease in intensity in the surface region (top 100 μm).

Figure 10 is a simulation for a drying latex dispersion (without cross-linker) and consists of two parts. The top part shows the water profiles as a function of time. These decrease gradually in concentration starting, as expected, from the film surface. The thinning of the coating as the water evaporates is also evident. The profiles are smooth. Although the water concentration is lower near the air surface, there is no skin layer as such forming. The total drying time is about 1 h, which is consistent with experiment. The lower part of the figure is the latex polymer content. It increases with time as evaporation proceeds and the coating becomes thinner. Eventually, the latex polymer fraction reaches unity and is spatially uniform. In this case, the latex polymer gives no signal and the mobile component is the water only. Consequently, the magnetization profiles follow the pattern of the water profiles. The upper part of figure can thus be compared directly to Figure 6. Again, a good comparison is seen. In both cases, magnetization profiles move down from the air interface and decrease in intensity to zero with time.

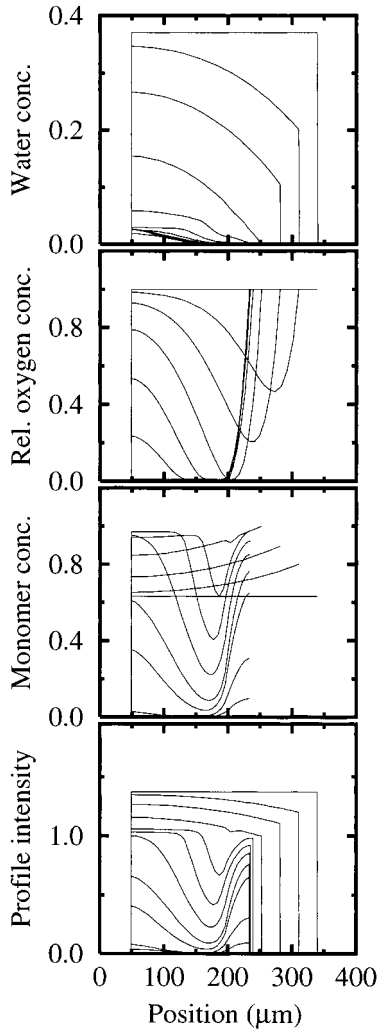

Figure 11. Simulated profiles for the drying and cross-linking of a wet latex coating (complete formulation) exposed to light (from the right of the plot) using the parameters given in the text. In all cases, the top square-shaped profile is the initial one. Subsequent profiles are shown at 10 min intervals until 80 min and then at 2 and 3 h. The plots (from top to bottom) are as follows: water fraction; fraction of active oxygen relative to the initial value; unreacted cross-linker monomer fraction; and magnetization (cf. Figure 8). To aid clarity, the upper edges of the profiles are not drawn in the central plots.

Table 1. Initial Concentrations of the Constituents Used in the Numerical Simulations

system	ϕ_w	ϕ_m	ϕ_o^0	photoinitiator fraction
reacting cross-linker only	0	0.98	10^{-4}	0.02
drying latex only	0.46	0.54	0	0
complete formulation	0.36	0.62	4×10^{-6}	0.02

Figure 11 shows the drying and cross-linking of a complete formulation. These simulations combine features of the two previous simulations. At the top is the water content. As in Figure 9, the thickness of the layer

decreases over time, and the concentration is lower at the surface. However, a distinct break of gradient in the profiles is now seen after 40 min when cross-linking in a middle layer sets in. Lower water concentration near the surface develops because the diffusivity of water in polymer is much less than in monomer.[3] This surface region with lower water content represents a "skin" layer. The second plot shows the active oxygen content. It decreases with time, most rapidly in the center of the coating. Near the surface, oxygen is replenished by the incident flux. Near the substrate, the light does not penetrate sufficiently to create enough radicals to consume the oxygen. The reaction of the cross-linker monomer (in the third plot) is initiated in the middle region of the coating as soon as the local oxygen content reaches zero. As before, cross-linking at the surface is enabled by monomer diffusion in the polymer. At the back, cross-linking is partially delayed until the light penetrates once the film is dry, although the monomer diffusion mechanism still operates. Finally, the bottom plot shows the expected magnetization profiles calculated as before. This plot can be compared directly to Figure 8. It captures the evolution of a decreased intensity in the center of the coating, which was found in experiments.

The parameters in the simulations have been made as self-consistent as possible and have been independently verified, as far as is possible. All the simulations were run using the same set of rate constant parameters: $k_d = 10^{-6}$ s^{-1}, $k_p = 2 \times 10^{-4}$ s^{-1}, and $k_t = 10^6$ s^{-1}. These values are consistent with typical values in the literature.[20,32] However, in the case of k_d, this is not a fair comparison because I_0, the surface light intensity that accompanies it, is a free parameter. In each simulation, $I_0 = 1$. The characteristic light attenuation length, z_0, is taken to be 50 μm as long as the film has not dried, $\phi_w > 0$. This value is fractionally larger than that suggested by the data already shown in Figure 3, because the value of z_0 is expected to increase as ϕ_w increases. In the absence of water when $\phi_w = 0$, $z_0 = \infty$.

The surface oxygen flux, O, is an adjustable parameter taken as 10^{-12} ms^{-1}. The free evaporation rate of water, E, is taken as 5×10^{-8} ms^{-1}, as determined from our gravimetric measurements shown in Figure 3. Finally, the requisite diffusion coefficients are chosen as $D_{w,m} = 3 \times 10^{-11}$ m^2 s^{-1}, $D_{o,w} = D_{o,m} = D_{o,p} = 3 \times 10^{-12}$ m^2 s^{-1}, and $D_{w,p} = D_{m,p} = 3 \times 10^{-13}$ m^2 s^{-1}, where the subscripts w, m, p, and o stand for water, unreacted cross-linker (monomer), reacted cross-linker (polymer), and active molecular oxygen, respectively. The values of the self-diffusion coefficients of water and of the cross-linker in a 50 vol % aqueous solution were both measured independently using spectroscopically resolved pulsed-gradient spin-echo diffusometry[24] and found to be 4.02×10^{-9} and 3.2×10^{-9} m^2 s^{-1}, respectively, which is comparable to the literature value for water.[35] The latter value is surprisingly large, considering that the molecular size of the cross-linker is 2 orders of magnitude greater than that of water. Note that these measured values are much larger than $D_{w,m}$ as used in the simulations. One reason for the difference is that pulsed-gradient spin-echo diffusometry measures self-diffusivities, while the simulation requires mutual diffusivities. Another is that the measurements correspond to a specific and rather high water concentration prior to any film formation. Without the consideration of the concentration dependence of the diffusion constants, the values in the simulation must reflect an average over the course of the entire drying and cross-linking processes.

As already seen, these values of the parameters produce theoretical profiles in general accordance with the data. While they should under no circumstances be considered to be *fits* to the data, the profiles capture all of the general trends observed experimentally. The values of the parameters cannot be changed by large factors without incurring large and obvious discrepancies of profile shape compared to the presented experimental data.

There is one exception, however, in which agreement is not obtained: the drying of the complete formulation but without photoinitiator, the experimental data for which are shown in Figure 7. This data set reveals simplifications, in the analysis, which, although not detracting from the relevant physics, mask subtleties evident in further experiments. The signal intensity of the water was assumed to be constant over time and with changing concentration. Mobile water has a large self-diffusion coefficient and a long spin−lattice relaxation time, T_1. Self-diffusion attenuates the water signal at later echo times when recorded in a strong magnetic field gradient. Spin−lattice relaxation also attenuates the signal, if the repetition time between measurements is short. Both factors apply here. As the water becomes less mobile with decreasing volume fraction and concomitant confinement between the latex particles, T_1 decreases and the signal intensity per unit volume of water increases, apparently faster than the total volume decreases. With reference to Figure 7 in particular, this effect accounts for the unexpected *increase* in signal intensity occurring during the earlier period of drying and the subsequent reversal of the MR profile spatial gradient.

Similar comments apply to the cross-linker monomer, but the effects are not so strong. The monomer swells and plasticizes the latex particles, according to hardness and viscoelastic measurements.[36] We have found that unswollen latex particles contribute negligible signal intensity whereas swollen particles, as in Figure 5, give a measurable signal. In the analysis presented so far, the cross-linker and latex particles have been considered as a single component. Consideration of the monomer and latex separately introduces an extra component into the analysis and severely complicates the interpretation of the MR intensity. Moreover, the addition raises the required number of necessary diffusion coefficients from six to ten. Ten is a substantial number of unknown parameters, which can no longer be considered in the simple manner adopted so far. Differing latex polymer and cross-linker monomer diffusivities can give rise to spatial gradients in these components during drying, which, in turn, would be reflected in the spatial magnetization. There is some evidence for this in the way in which the profile pivots toward its final uniform shape at longer times in Figure 7.

6. Concluding Remarks

We have shown that magnetic resonance profiling is now sufficiently well developed to be of significant use in the study of film formation of photoinitiated latices. The method produces depth-resolved composition and mobility profiles that can be used for direct comparison with numerical simulations. We have developed a model combining the principles of water evaporation, mutual

diffusion of the various components, photoinitiated free radical polymerization, oxygen inhibition of free-radical reactions, and oxygen ingress. This model is able to reproduce the characteristic trends in the experiments reported here. Notably, it is able to explain the highly nonuniform drying and cross-linking in the depth of the latex films. We conclude that both oxygen inhibition and latex turbidity present real obstacles to obtaining uniformly cross-linked, waterborne coatings in systems such as this one.

The model is also able to explain the features of experiments not reported here. For instance, if oxygen ingress into the cross-linker is prevented, then cross-linking is uniform, but there is still an induction period due to dissolved molecular oxygen. Or if light is transmitted through the glass substrate and shone on a complete formulation from behind, cross-linking is faster along the interface while the effects of oxygen inhibition at the air surface persist.

In the work described here, only simple echo sum data have been presented. The separate analysis of multiple echoes in a train would yield considerably more molecular dynamic contrast[13] than we have chosen to exploit. In closing, we note that the use of this recently developed magnet design need not to be restricted to the study of film formation in cross-linking systems. Indeed, we have already applied it to the film-formation process of alkyd emulsions[35] and, in another field, to the diffusion of water into human skin.

Acknowledgment. We gratefully acknowledge funding from the UK Engineering and Physical Sciences Research Council for the design and construction of the MRI magnet at the University of Surrey. We are also grateful for funding from Arvid Lindgrens Fond för Färgforskning (for the travel and accommodation expenses of M.W.) and from the European Union through the BRITE-EURAM III Program (Contract BRPR CT98 0646). We appreciate experimental contributions from J. M. Salamanca and Drs. E. Ciampi and A. Barry (University of Surrey).

References and Notes

(1) Winnik, M. A. *Curr. Opin. Coll. Interface Sci.* **1997**, *2* (2), 192.
(2) Keddie, J. L. *Mater. Sci. Eng. Rep. R* **1997**, *21*, 101.
(3) Routh, A. F.; Russel, W. B. *Langmuir* **1999**, *15*, 7762.
(4) Feng, J.; Pham, H.; MacDonald, P.; Winnik, M. A.; Geurts, J. M.; Zirkzee, H.; van Es, S.; German, A. L. *J. Coat. Technol.* **1998**, *70* (881), 57.
(5) Pham, H. H.; Winnik, M. A. *Macromolecules* **1999**, *32*, 7692.
(6) In thermoplastic latex systems, there is little *direct* experimental evidence for a skin layer. Some evidence of this layer is provided, however, in: Okubo, M.; Takeya, T.; Tsutsumi, Y.; Kadooka, T.; Matsumoto, T. *J. Polym. Sci., Polym. Chem. Ed.* **1981**, *19*, 1.
(7) Vanderhoff, J. W.; Bradford, E. B.; Carrington, W. K. *J. Polym. Sci.* **1973**, *41*, 155.
(8) Young, R. J.; Lovell, P. A *Introduction to Polymers*, 2nd ed.; Chapman & Hall: London, 1991.
(9) Mansfield, P.; Granell, P. K. *J. Phys. C: Solid State Phys.* **1973**, *6*, L422.
(10) Lauterbur, P. C. *Nature* **1973**, *242*, 190.
(11) For a good overview of the applications of MRI in materials science, see: *Spatially Resolved Magnetic Resonance*; Blümler, P., Blümich, B., Botto, R., Fukushima, E., Eds.; Wiley-VCH: Weinhein, Germany, 1998.
(12) Ciampi, E.; Goerke, U.; Keddie, J. L.; McDonald, P. J. *Langmuir* **2000**, *16*, 1057.
(13) Glover, P. M.; Aptaker, P. S.; Bowler, J. R.; Ciampi, E.; McDonald, P. J. *J. Magn. Reson.* **1999**, *139*, 90.
(14) McDonald, P. J.; Newling, B. *Rep. Prog. Phys.* **1998**, *61*, 1441.
(15) Blumler, P.; Blumich, B. *Rubber Chem. Technol.* **1997**, *70*, 568.
(16) Kimmich, R. *NMR Tomography, Diffusometry and Relaxometry*; Springer: Berlin, 1997.
(17) Wicks, Z. W., Jr. *Film Formation*; Federation Series on Coatings Technology: Blue Bell, PA, 1986.
(18) Crivello, J. V.; Narayan, R.; Sternstein, S. S. *J. Appl. Polym. Sci.* **1997**, *64*, 2073.
(19) Decker, C.; Nguyen, T. V.; Xuan, H. L. *Eur. Polym. J.* **1997**, *32*, 1319.
(20) Cook, W. D. *Polymer* **1992**, *33*, 600.
(21) Watts, D. C. In *The Setting Mechanisms of Dental Materials*; The Academy of Dental Materials: Richmond, VA, 1992; p 1.
(22) Decker, C.; Jenkins, A. D. *Macromolecules* **1985**, *18*, 1241.
(23) Decker, C.; Bendaikha, T. *J. Appl. Polym. Sci.* **1998**, *70*, 2269.
(24) Callaghan, P. T. *Principles of Magnetic Resonance Microscopy*; Clarendon: Oxford, 1991.
(25) Hisatake, K.; Tanaka, S.; Aizaw, Y. *J. Appl. Phys.* **1993**, *73*, 7395.
(26) Croll, S. G. *J. Coat. Technol.* **1986**, *58*, 41.
(27) Winnik, M. A.; Feng, J. *J. Coat. Technol.* 1**996**, *68*, 39.
(28) Routh, A. F.; Russel, W. B. *AIChE J.* **1998**, *44*, 2088.
(29) Crank, J. *The Mathematics of Diffusion*; Clarendon: Oxford, 1975.
(30) Onsager, L. *Ann. N. Y. Acad. Sci.* **1945,** *46*, 241.
(31) Curtiss, C. F.; Hirschfelder, J. O. *J. Chem. Phys.* **1949**, *17*, 550.
(32) Cowie, J. M. G. *Polymers: Chemistry and Physics of Modern Materials*; Intertext Books: Aylesbury, UK, 1973.
(33) Meeten, G. H. *Optical Properties of Polymers*; Elsevier Applied Science: London, 1986.
(34) Mills, R. *J. Chem. Phys.* **1973**, *77*, 685.
(35) Hellgren, A.-C.; Wallin, M.; Weissenborn, P.; McDonald, P. J.; Glover, P. M.; Keddie, J. L., submitted to *Prog. Org. Coat.*

MA000787D